Environmental Modelling and Software 197 (2026) 106816

Contents lists available at ScienceDirect

Environmental Modelling and Software

journal homepage: www.elsevier.com/locate/envsoft

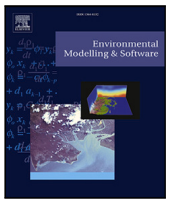

Modelling near-surface ice content and midwinter melt events in mineral soils

Élise G. Devoie [a,*], Renato Pardo Lara [b], Aaron Berg [b], William L. Quinton [c], James R. Craig [d]

[a] Department of Civil Engineering, Queen's University, Kingston, K7L 3N9, ON, Canada
[b] Department of Geography, Environment and Geomatics, University of Guelph, Guelph, N1G 2W1, ON, Canada
[c] Cold Regions Research Centre, Wilfrid Laurier University, Waterloo, N2L 3C5, ON, Canada
[d] Department of Civil and Environmental Engineering, University of Waterloo, Waterloo, N2L 3G1, ON, Canada

ARTICLE INFO

Dataset link: https://github.com/egdevoie/InterfaceModel.git, https://opensource.org/license/mit, https://doi.org/10.20383/101.0116

Keywords:
Seasonal freeze/thaw
Freeze/thaw modelling
Cold region hydrology
Midwinter melt
Semi-analytical modelling

ABSTRACT

Over winter freeze–thaw events are notoriously difficult to represent in hydrologic models and have serious implications for the hydrologic function of intermittently freezing regions. Changing climate is leading to more frequent mid-winter thaw events. Midwinter thaw events are often the cause of flooding due to the combined impacts of snowmelt, precipitation, and limited soil infiltrability. A numerically efficient, semi-analytical coupled thermal and mass transport model is presented that represents the ice content of near-surface soil, and reports the depth of freezing/thawing. The model tracks pore ice formation and mean soil temperature in terms of enthalpy. It is tested against data collected in Southern Saskatchewan and is shown to capably reproduce field observations of frozen, thawed or transitioning soils. This numerically efficient model can be incorporated into regional hydrologic models where it is expected to improve predictions of soil ice content, leading to improved estimates of over-winter streamflow and flood potential.

1. Introduction

It is well established that anthropogenic climate change is leading to increased variability in climate and more frequent and severe weather events (Pörtner et al., 2019). With a changing climate, the intermittent frozen soils ubiquitous of Southern Canada and Northern United States have been observed to be affected by more frequent midwinter melt events (Williams et al., 2015).

Midwinter melt events followed by freeze-back have been found to increase the runoff ratio of landscapes, yielding greater than expected runoff following midwinter melt and freeze-back events (Hyman-Rabeler and Loheide, 2023). Midwinter melt events reduce the hydraulic conductivity of frozen soils by increasing the total water content, observed to increase tortuosity and flow-path length in frozen soils, and decrease active porosity (Granger et al., 1984). Observations of depression-focused infiltration of snowmelt water in the Canadian prairies show an evolution in runoff ratio in which midwinter melt events have lower runoff ratio than the subsequent spring melt (Hayashi, 2013; Pavlovskii et al., 2019). In agricultural fields, this process results in limited capacity to infiltrate the snowmelt, leading to high runoff events, high peaks in the freshet period of the hydrograph, and lower than expected spring soil moisture (Van der Kamp et al., 2003). In restored grassland sites, Van der Kamp et al. (2003) found that the infiltration of snowmelt water was sufficient to avoid surface ponding. This infiltrability was attributed to the presence of macropores and preferential flow paths which are disrupted by tillage in agricultural fields. At large scales, preferential flow paths through macropores dominate the infiltration into soils, and field observations indicate that runoff partitioning is mediated by infiltration into frozen soils through macropore systems (Mohammed et al., 2019).

In many hydrologic models, frozen soils are either treated as strictly impermeable surfaces for the entire winter period (Niu and Yang, 2006) or empirical or parametric (empirical models fit to specific field conditions) models are used to address the changes in infiltrability due to ice content over the winter months (Luo et al., 2003). In systems that are generally quiescent over the winter months, empirical models of over-winter processes have been found to be adequate (Luo et al., 2003). This has motivated the use of empirical or parametric models such as those presented by Zhao and Gray (1999), Hayashi et al. (2007), Lundin (1990), which can be transferable to other study sites through parameter tuning based on field data, but are not applicable in non-stationary systems such as those affected by changing climate (Pavlovskii et al., 2019). Empirical approaches lead to an inability to accurately report the soil moisture, thermodynamic state, hydraulic conductivity, infiltrability, and water storage of non-stationary systems without field measurement.

* Corresponding author.
E-mail address: elise.devoie@queensu.ca (É.G. Devoie).

https://doi.org/10.1016/j.envsoft.2025.106816
Received 3 February 2025; Received in revised form 31 October 2025; Accepted 3 December 2025
Available online 5 December 2025

Alternatively, many land surface schemes (e.g., Verseghy (2000)) explicitly simulate the full soil energy balance with freezing, which is typically accompanied by significant computational cost. Even in these models where the representation of freeze/thaw is based on simplified relationships including 1-D solutions to the Stefan problem (Woo et al., 2004; Yi et al., 2006), the applicability of the solutions in heterogeneous landscapes is limited, and models fail to capture seasonal events such as snowmelt, runoff partitioning, or midwinter melt (Slater et al., 1998; Cuntz and Haverd, 2018), limiting their capacity to accurately represent soil ice content and permeability. The explicit representation of soil ice content is included in some hydrologic models, especially those applied in permafrost regions (e.g. Luo et al. (2003), Pomeroy et al. (2007), Wang et al. (2010, 2017)). The accurate representation of frozen soils, including the coexistence of frozen and liquid water, improves hydrologic prediction in these regions (Niu and Yang, 2006), both for empirical and even more so for physically-based models (Wang et al., 2010; Pomeroy et al., 2007; Qi et al., 2019). Many current software tools including FEFLOW-FTM, SUTRA-ICE, SMOKER, and Cast3M explicitly model coupled heat and mass transport in a finite element mesh with the capacity to model local impacts of freeze/thaw on groundwater systems in great detail (McKenzie et al., 2007; Diersch, 2013; Grenier et al., 2013; Molson and Frind, 2015; Rühaak et al., 2015). However, physically-based coupled thermal and mass transport models are notoriously demanding computationally, and the representation of freezing and thawing of pore water, and its migration due to temperature gradients often increases computational time more than an order of magnitude, and can lead to instabilities and non-convergence of models (Wang et al., 2017). Due to these limitations, existing freeze/thaw models are inappropriate to inform watershed-scale surface water models.

We here propose a semi-analytical physical model that efficiently predicts freeze/thaw processes and ice contents in soils during midwinter melt and other short-duration freeze/thaw events that are currently not well captured by empirical models. As such, this model will fill the substantial gap separating physically-based, discrete continuum models from models that are purely empirical. The objectives of this paper are to (1) extend the methods developed for organic soils with permafrost by Devoie and Craig (2020) to mineral soils without permafrost, (2) evaluate the extended model against a continuum model benchmark, and (3) apply the model to intermittently frozen soil data collected at the Kenaston Field site in Saskatchewan, Canada, with a focus on short-duration freezing in the near-surface soil. Though the interface model is a front tracking model, the aim of this study is to evaluate its ability to efficiently predict freeze/thaw events to inform hydrologic models.

2. Methods

A combination of two modelling techniques and field-based measurements are used to establish the validity of the proposed interface model for the representation of freeze and thaw events in seasonally frozen mineral soils, especially for short duration midwinter melt events. Further model validation from Devoie and Craig (2020) is included in appendix E . Model governing equations are described in appendix A, while model parameter definitions and values are summarized in appendix D.

2.1. Field

2.1.1. Field data

Soil moisture, temperature and precipitation have been monitored at 22 stations of the Kenaston Network located in the Brightwater Creek basin, east of Kenaston, SK, Canada (Tetlock et al., 2019). This is predominantly an agricultural region, dominated by annually cropped fields with some grazing land and without irrigation (Tetlock et al., 2019). The instrumented monitoring network spans 40 km^2, with most of the instrumentation within a flat 10 km^2 sub-region with slopes of less than 2%. The sites cover a soil textural composition of 10.5 - 61.7% sand, 31.2–72.4% silt and 1.2–41.1% clay, for the base computational test, a representative soil (from Kensaton site 1) of 28% sand, 53% silt and 19% clay was used (Pardo Lara et al., 2020, 2021). The mean annual air temperature in this region is 8 °C, and in the last three decades the mean annual precipitation has been 400 mm of which approximately 30% falls as snow (Meteorological Service of Canada, 2012). The catchment is semi-arid, and fluctuations in soil moisture follow a seasonal pattern (Burns et al., 2016), though some fill-and-spill and non-contributing areas are documented where water ponds in sloughs instead of contributing to the basin outflow (Shook et al., 2013).

Soil moisture was measured using "HydraProbes", commercially available electromagnetic sensors that report liquid water content from permittivity and temperature measurements (Seyfried and Murdock, 2004). The sensors have 4 metal tines which are 3 mm in diameter and 57 mm long. The zone of influence of the probe ranges approximately from 4.0 x 10^4 mm^3 to 3.5 x 10^5 mm^3, with a radial range of approximately 13 to 35 mm (Pardo Lara et al., 2021). Given the measurements from these probes installed at depths of 5, 20, and 50 cm below the ground (Pardo Lara et al., 2020), it is assumed that the near-surface probe is sensitive to water content in the top 50 ± 35 mm of soil, and this near-surface layer is used to report the frozen, thawed, or transitioning state of the soil surface. Soil temperature was measured alongside soil moisture and permittivity (as part of the soil moisture measurement) at three depths: 5, 20 and 50 cm below the ground surface (Burns et al., 2016). Precipitation was also measured at each site using tipping bucket rain gauges. All data was collected at 30-minute intervals (Tetlock et al., 2019).

2.1.2. Kenaston data-driven estimate

A field-based approach to determining the frozen or thawed state of the soil was used to generate validation data for the interface model discussed above. This approach uses soil permittivity and temperature data to establish a site-specific freezing point. The freezing temperatures were estimated using a logistic growth model fit to the soil freezing curve, as detailed in Pardo Lara et al. (2020). This allowed consistent estimates of soil pore water as thawed, frozen, or undergoing phase change based upon the observation data. These temperature and soil moisture data were used to validate the predicted freeze/thaw state from the interface model by specifying the field-data based freeze/thaw/transition flag. Though temperature and soil moisture data are available, the sensors are only proven to indicate if the soil is frozen, thawed or undergoing phase change (Pardo Lara et al., 2020). Calibrations reporting exact ice and liquid water content are not available, and merit further investigation.

2.2. Model

2.2.1. Interface model

The interface model is a semi-analytical solution to the heat equation coupled to an equilibrium solution to a mass balance relationship based on the van Genuchten pressure-saturation relationship. In this interface-based model, the depth of the frozen-unfrozen interface is treated as a state variable. This interface model water first presented in Devoie and Craig (2020), but is extended to represent seasonally frozen mineral soils. The heat transport includes both heat flux due to conduction ($\dot{Q}$) and advection (where $\dot{m}$ is the mass flow rate). These relations are presented below, while each term in the relation is described in appendix D.

$$\frac{dE}{dt} = \dot{Q}_{in} - \dot{Q}_{out} + \dot{m}_{in} e_{in} - \dot{m}_{out} e_{out}$$

$$c_{p,b}\rho_b \frac{\partial \bar{T}}{\partial t} = \lambda_b \left(\frac{\partial T}{\partial z}|_{top} - \frac{\partial T}{\partial z}|_{bottom} \right) + I\,\Delta t c_{p,w}\rho_w (T_{precip} - T_f) - q_{bottom}(T_{bottom} - T_f)\rho_w c_{p,w}$$

This set of equations can be solved semi-analytically in the surface layer where ΔT_s^t refers to the change in temperature of the surface

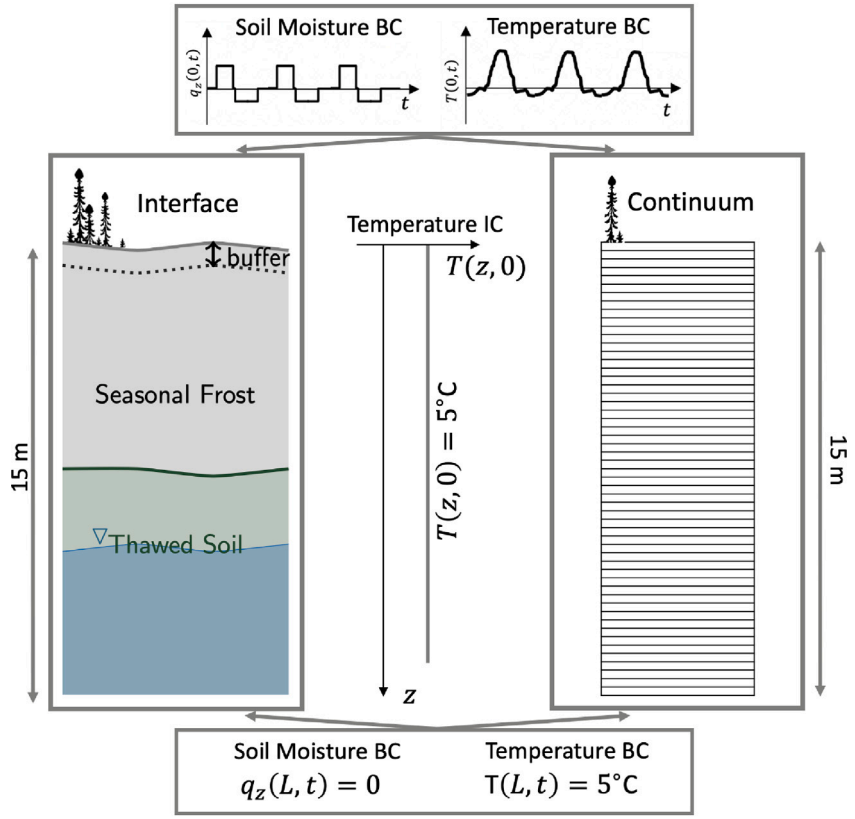

Fig. 1. Schematic diagram showing model domain, boundary conditions (BCs) and initial conditions (ICs). The interface model (left) tracks the buffer layer (where fractional ice content is permitted) and the interface between frozen and thawed soil. The water table depth is also computed separately and updated through an equilibrium mass balance. The finite volume continuum model (right) used here for comparison uses operator splitting to solve the coupled PDEs describing heat and mass transport in 1D. Not shown is the initial water table position of the model 1 m below the ground surface (ψ = 1 m, water table at $z = 1$).

between timestep t and $t + 1$, and the boundary condition at the base of this layer is defined by a fixed temperature of 0 °C if the system is freezing or thawing, or a specified temperature if the system is fully thawed.

$$T(z,t) = \sum_{n=1}^{N} \Delta T_s^n \left(1 - \frac{z}{L} - \sum_{j=1}^{\infty} a_j \sin(\omega_j z) e^{-\alpha\omega_j^2 (t-t^n)}\right)_n$$

A similar relation but with fixed temperature as the boundary conditions is specified in the other soil layers, and are updated according to seasonal freeze/thaw cycles congruent with the system shown in Fig. 1.

The interfaces between the soil layers are updated using the temperature gradients at element interfaces to calculate the heat flux across these interfaces. In order to approximate this gradient, an analytical solution to the heat equation (without phase change as this process only occurs at the interface) is used in each domain element. There are three such distinct profiles for each type of element. These solutions are outlined in appendix A.

The movement of the (sharp) interfaces is determined by the fluxes based on temperature gradients and thermal conductivity. The change in interface position (z_i) is given by:

$$\frac{\partial z_i}{\partial t} = \frac{1}{\lambda_f(\theta_w - S_{res})\rho_w} \Delta q|_{z=z_i}$$
$$= \frac{1}{\lambda_f(\theta_w - S_{res})\rho_w} \left(\kappa^+ \left(\frac{\partial T}{\partial z}\right)_{z=z_i^+} - \kappa^- \left(\frac{\partial T}{\partial z}\right)_{z=z_i^-}\right)$$

Where z is depth, and $\kappa^{\pm}$ is the thermal conductivity of the element above (+) or below (-) the interface.

Mineral soils with lower hydraulic conductivity challenge the equilibrium representation of the water balance, leading to model modifications to include transient infiltration and evapotranspiration. The numerical implementation details and derivation are included in appendix C.

Given these modifications, the interface model reports the water table position as well as the freeze/thaw fronts in the subsurface (see Fig. 1). The updated model also includes a surface "buffer" layer of fixed thickness that may contain a fractional ice content (liquid water in excess of the residual unfrozen water content and solid water coexisting in soil pores). This enables a better approximation of the near-surface soil behaviour, and prevents the non-physical formation of thin freeze/thaw interfaces. In this work the buffer layer is specified to be 85 mm, based on the zone of influence of the field measurements (Section 2.1.1) of the near surface unfrozen water content used for model validation. This layer limits the fractional ice content to the near-surface, and the model is otherwise purely front-tracking with user-specified residual unfrozen water content. The limitations of this front-tracking approach are discussed in Section 4.3. The interface model is appropriate for representing the total ice content in the soil column (without its exact spatial distribution), and estimating the freeze/thaw state of the near surface soil as is needed for predictions of soil infiltrability.

2.2.2. Continuum model

To validate the details of its formulation, the interface model was directly compared to a coupled solution of the unsaturated Richards' equation and an energy balance including conduction, advection, and phase change terms, solved via a finite volume method with operator splitting, as presented previously in Devoie et al. (2019). The governing

equations are presented in appendix A. This detailed numerical solution allows us to assess the impact of the simplifying assumptions made in the interface model to ensure that the model adequately represents the physical processes. Identical initial conditions and boundary conditions were used in both models (described in Section 2.2.3), and a spatial discretization of 1 cm and 2 cm were compared, both using 1 h time steps in the continuum model. The same soil parameters were used for this model as were used in the interface model, with the addition of a linear soil freezing characteristic curve (SFCC) for a (theoretical) freezing range of −0.005 to 0 °C. This narrow range was chosen to match the interface model which does not include an SFCC as it tracks a sharp interface without a slushy region.

2.2.3. Initial and boundary conditions

For comparison with field data, the model domains of both models were extended to a depth of 15 m, using a fixed soil temperature of 5 °C at the base of the profile, consistent with the mean annual soil surface temperature of 5 °C, and the negligible geothermal gradient of 0.002 °C/m (Majorowicz and Grasby, 2021). This temperature is in agreement with data collected in Saskatoon (about 85 km from the study site), where the average soil temperature at 3.0 m was 6 °C, decreasing with depth, though there was still evidence of seasonal variation (Wittrock and Dunn, 2016). An initial water table position was assigned at 1 m below the ground surface, based on the water table data measured in the field in early spring. Mass flux at the surface was applied seasonally, with an average ET rate (−2.07 mm/d) applied in spring/summer and an average recharge rate (2.42 mm/d) in the fall. The 15 m depth was specified to be well below both the expected minimum water table depth and the depth of zero annual amplitude in temperature, but the precise choice of 15 m is arbitrary: one of the benefits of the semi-analytical model is that a large vertical extent does not increase computation time. The net mass flux through the surface was zero annually. A no-flow boundary condition was assigned at the base of the soil column to represent the near-impermeable unweathered till underlying this system, and the competent bedrock beneath that (Shaw and Hendry, 1998). The surface temperature boundary condition was estimated based on soil temperature collected at a depth of 5 cm in the field sites near Kenaston, and forced with a seasonally cyclic moisture boundary condition (reported in Section 3) as direct application of the infiltration flux data collected in the field precluded convergence of the continuum model used for benchmarking due to numerical instabilities. The soil column was initialized to a thawed uniform temperature of 5 °C, and the freeze/thaw discriminant temperature was assigned based on the specific freezing point depression determined from the field data, ranging between 0 and -0.4 °C (Pardo Lara et al., 2020). Simulations were started in the summer of 2012, except at sites 16 and 18 which were started in summer 2013 due to lack of data. All simulations were run for a duration of 5 years, with associated computational time of 11 s for each simulation. Because of the moving interface, there is no spatial discretization of the interface model, however there is temporal discretization, and the simulations reported here are run with a 1 h timestep for comparison with the finite volume model in Fig. 3 and a 1 day timestep otherwise. Other soil parameters were homogeneous and independent of depth, and are summarized in table 1 in appendix B both for organic and mineral soils.

3. Results

The simulation of seasonal freeze–thaw is first verified via a numerical benchmarking study in an unsaturated system typical of mineral soils in the semi-arid climate of Southern Saskatchewan. Boundary conditions and soil parameters were obtained from field data, but no direct measurements of freeze/thaw are available for the benchmark; these tests are purely to demonstrate numerical accuracy of the method. Finally, the interface model predictions are directly compared to the data-derived freeze/thaw status at sites in the Canadian prairies to evaluate the practical efficacy of the method.

3.1. Kenaston

The model was evaluated based on a five-year simulation of field data collected at site 1 of the Kenaston Soil Moisture Network, using a 15 m vertical domain and initial and boundary conditions as detailed in Section 2.2.1. Fig. 2 shows the comparison between the continuum model, interface model, as well as field data indicating the 'frozen period'. A synthetic boundary condition for water flux at the surface was necessary for the convergence of the continuum model, with which the interface model shows excellent agreement in Fig. 2(a). The shaded grey areas in Fig. 2(b) indicate the period over which the near-surface soil (approximately 40–85 mm) at the field site was frozen. This data is drawn directly from field measurements using the methodology outlined in Section 2.1.1, and compares favourably with the reported freeze/thaw timing. The use of field data resulted in an RMSE of 0.04 between the total ice content simulated by the interface model and continuum model, yielding excellent agreement. The ice content in the interface model is calculated as a sum of the total water content in the frozen layer, less the residual unfrozen water content specified by the soil texture. The continuum model provides ice content as a state variable, computed based on temperature and the specified SFCC. The interface position in Fig. 2(c) tracks the zero degree isotherm relatively well, though the interface position is slightly deeper when compared to the discretized model. This difference may be attributed to the equilibrium distribution of soil moisture in the interface model, resulting in slightly higher thermal conductivities than in the discretized model (especially for frozen soils) 4.5. The performance of the interface model is however significantly better than a simple degree-day method from Fox (1992) which significantly under-estimates the thawing front, shown in black in Fig. 2(c). More recent advances have focused on the development of computationally demanding numerical techniques, while the degree-day model presented here has been refined based on work presented in Woo et al. (2004), Hinkel and Nicholas (1995), for the representation of multiple fronts. Further work on front-tracking models in Hayashi et al. (2007) is the precursor to this work, where many of the simplifications in that model (neglecting sensible heat, applying a cumulative average temperature) have been lifted in the approach presented here. The simulation was re-run using finer spatial and temporal discretization in the continuum model (shown in Fig. 3) to capture the exact timing of a specific freeze/thaw event, which was not captured using the model setup used to simulate the entire period (5 cm spatial discretization and 3 minute timestep).

The comparison of the interface and continuum model for the short-duration event in Fig. 3 was generated using the same model configuration as Fig. 2, but with finer spatial and temporal discretization of both models. The comparison of computational efficiency can also be established in Fig. 3 as the continuum model run took 2 h and 22 min (in blue) while the interface model (red) only took 4.5 s for the same size time step and simulation setup, 3 orders of magnitude faster than the continuum model. The performance of the interface model is arguably better than the continuum model: when the spatial discretization of the continuum model is refined, it tends towards the interface model solution. Larger spatial steps lead to a lack of identification of the freezing event in the continuum model, and smaller spatial (and associated temporal) discretization was computationally impractical. This is likely due to the information loss in the discretization of the spatial and temporal domain, in which larger steps are more challenging to resolve numerically, resulting in the steep transitions seen (e.g. at day 8 in the dz = 2 cm case). As the spatial and temporal steps decrease, the solution tends towards the "true" analytical solution, and the relations are smoother. The interface model is not a discretized model, so it is free of this source of information loss and error. Neither model captures the initial freezing event near day 7, likely due to the choice

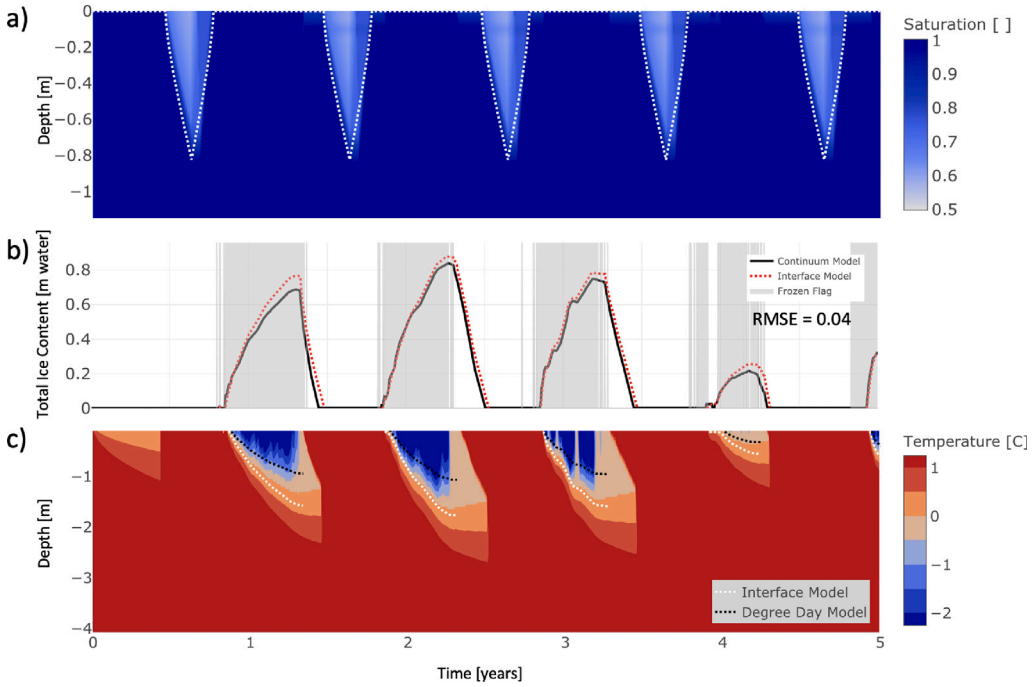

Fig. 2. (a) Comparison of water content for interface and continuum model (b) comparison of total ice content for continuum model (black), interface model (red) and field-based near-surface frozen flag (shaded grey) and (c) contour plot of continuum model temperature with freeze/thaw interface position from interface model superimposed in white dashed line. Degree day model from Fox (1992) in black dashed line. Field-data driven with surface water flux approximated as seasonally uniform due to stability constraints for continuum model, soil texture data drawn form Kenaston Site 1 in Table 1 of appendix D.

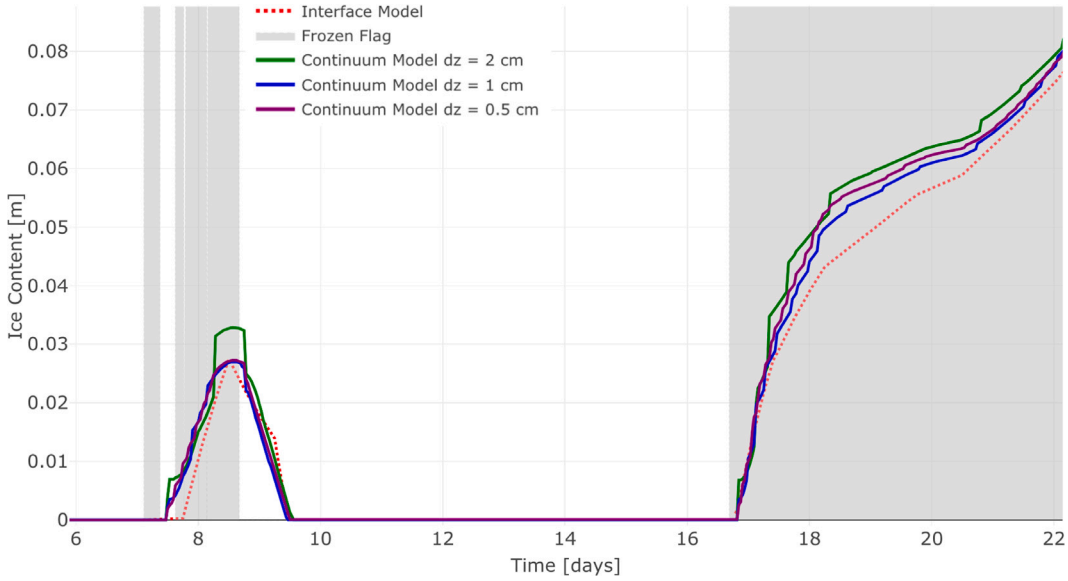

Fig. 3. Short duration freeze/thaw initiation. Comparison of interface model (with 6 h timesteps) to continuum model with timesteps chosen to satisfy convergence criteria given spatial discretization, on the order of minutes. This short duration initiation of freezing results in a small quantity of near-surface ice, hence the small total ice content. Spatial steps larger than 2 cm do not capture the near-surface freezing event in the continuum model. Model convergence is assumed based on the similarity between the 1 cm and 0.5 cm simulations. Grey shaded regions indicate soil freezing according to the field-data. Soil texture data drawn form Kenaston Site 1 in Table 1 of Appendix D.

of (theoretical) freezing point depression (−0.005 ° C) and the freezing range between 0 and -0.01 ° C for the interface and continuum models respectively. Subsequent figures generated using only the interface model without continuum model comparison use the freezing point depression determined from field measurements at the given field sites in order to better capture such events.

3.2. Midwinter melt

The benchmarked interface model was applied to a total of 22 sites in which subsurface temperature and soil moisture were recorded for a duration of 4–6 years between 2014 and 2020. In 10 of these 22 sites, clear mid-winder thaw events were identified, in which the soil

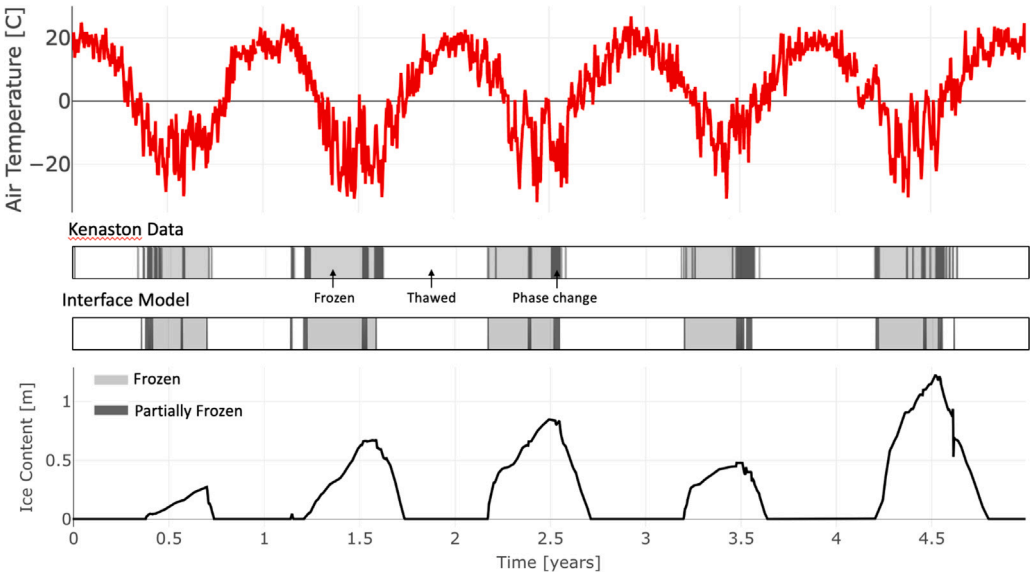

Fig. 4. Comparison of Kenaston field-data and interface model generated near-surface ice content indicating phase change (dark grey) and frozen soil (light grey). Total ice content from interface model shown along bottom axis. Daily average air temperature for the period shown in red. Soil texture data drawn from Kenaston Site 3 in table 1 of Appendix D.

temperature warmed above 0 °C. The interface model was run using surface soil temperature data available at these sites, and compared to the freeze/thaw flag extrapolated from the field data. Here a second "transition" flag was added to the field data representing soils undergoing phase change; if the surface layer of soil contained fractional ice content based on its permittivity this flag was activated. This flag is shaded in dark grey in the subsequent figures, while entirely frozen near-surface soils (with only residual water content) were assigned a "frozen" flag, depicted in light grey and thawed near-surface soils were left as white bands. Two separate flags were also implemented in the model — the first "transition" flag representing fractional ice content in the near-surface, and the second "frozen" flag indicating residual water content only, assigned the same colours as the field data. Sample results for the entire 5 year simulation at Kenaston site 3 are shown in Fig. 4, showing agreement between the interface model and data-extrapolated freeze/thaw timing. Two error metrics are used to compare the simulated and observed near-surface ice content. The first indicates the overall agreement between the modelled and measured data including frozen, thawed and transitioning states. For the data in Fig. 4, the agreement is 92%, indicating that the measured and modelled soils did not have the same freeze/thaw state only 8% of the time. The second metric was conceived to identify the effectiveness of the interface model at identifying frozen soils, and so it compares the soil state only when the measured field data is frozen, and does not take into account partially vs. completely frozen soils. For this study case, there is 91% agreement, indicating that the interface model incorrectly identified frozen soil as thawed 9% of the time.

4. Discussion

4.1. Interface model limitations

The interface model used in this study is a front tracking model, and its greatest limitation is therefore that it does not have the capacity to represent a slushy zone beyond the buffer layer. It does not use a soil freezing characteristic curve (SFCC), and it therefore will not be as robust as a continuum model when detailed information on the fractional ice content is needed. This is especially true for soils with SFCCs having a wide temperature range such as clay-rich materials. Future work integrating a linear SFCC into this model is planned, but more complex functional forms of SFCCs prevent the system from being solved analytically. The authors also caution against the use of this model in small-scale systems with significant groundwater recharge or discharge, as these processes depend on the detailed knowledge of distributed soil ice content to calculate fluxes. The interface model is however a good approximation of reality in sandy, coarse-grained soils where the SFCC is quite steep and the slushy zone is limited. It is also a valuable tool in the case of large-scale hydrologic simulations, which are limited by computational efficiency. In these cases, the approximation of freeze/thaw state in the near-surface provided by the interface model is superior to the current low-fidelity empirical models, as seen in Fig. 2(c).

Similarly to both empirical models and continuum representations, this model requires near-surface soil temperature as an input. Unlike air temperature, these values are not widely available, and for cases in which these data are unavailable a surface energy balance mode including snowpack representation would be required. Several existing models could be implemented, depending on the purpose of the model and data availability. In data-scarce regions is to apply a gridded land surface model which includes snowpack representation, and extrapolate soil surface temperatures for the region of interest. Though it is known that these models include bias (Wang et al., 2016), this can often be corrected using the closest recorded station data, and it is often a more effective estimation technique.

4.2. Model evaluation: Sensitivity analysis

The formulation of the interface model presented here is informed by many field measurements, but some parameters were estimated or inferred, including the residual unfrozen water content, θ_{res}, the thickness of the buffer layer, h, the total depth of the domain, L, and the freezing point depression, which was defined by the original analysis in Pardo Lara et al. (2020). While the model is affected by the selection of all input parameters summarized in the table in appendix B, the impact of these estimated or inferred parameters on ice content and timing of freezing onset is relevant to assess the robustness of the model formulation. A one-at-a-time (OAT) sensitivity analysis is performed on these model parameters, and the sensitivity to each, alongside their original value, are presented in Table 1. The sensitivity to ice content was established by fitting a linear regression to the total

Table 1
Sensitivity of interface model simulated ice content and initial freeze date to selected model inputs. Sensitivities followed by an (*) indicate the linear regression had an R^2 value greater than 0.5. The normalized sensitivity is presented, which is the product of the absolute sensitivity and the range of reasonable values (column 3).

Parameter	Original	Range	Sensitivity Ice [m^3]	Sensitivity Freeze Date [day]
Buffer layer thickness, h	0.0085 [m]	0.0005–0.01	581.5*	15.0
Domain length, L	15 [m]	5–50	0*	0*
Residual water content, θ_{res}	0.01 [–]	0.001–0.1	−80.8*	0*
Freezing point, T_f	[−0.44 °C]	0–−2	−613.6*	17.8*

ice content simulated for the range of model simulations, and reporting the slope of the regression. The Freeze date sensitivity was a similar linear regression fit to the date of first freeze-up as a Julian date. The product of this sensitivity and the feasible range (column 3) is reported. Data were generated using the Kenaston Site 15 model configuration.

As anticipated based on model formulation, the simulated ice content and freeze/thaw initiation is independent of domain length. The model is most sensitive to the freezing point, and almost equally sensitive to the buffer layer thickness. An increase in buffer layer thickness causes an increase in estimated ice content and a delay in freezing onset as a longer delay is required to fully freeze the buffer layer. Meanwhile, a drop in freezing point leads to a decrease in ice content, and a later freezing onset as more energy is consumed as sensible heat, cooling the soil to the lower freezing point. Finally, as the residual unfrozen water content in the model increases, there is a minor increase in total ice content, perhaps due to a more rapidly advancing freezing front. This sensitivity analysis nonetheless indicates that the model is structurally robust, as any of the sensitivities reported are less than 10% of the total ice content modelled, and can be interpreted physically.

4.3. Model evaluation: Near-surface buffer layer

Fig. 4 demonstrates agreement in the timing of broad seasonal events between the modelled data and data collected in the field, and Fig. 5 shows a more detailed view that distinguishes the typical seasonal freeze/thaw (i.e. freeze in the fall/early winter and thaw in the spring) from midwinter melt events. The interface model is highly effective in detecting the timing of freeze/thaw initiation, however the freeze/thaw transitions of the near-surface buffer layer tend to occur sooner than in the measured data (Fig. 5 & 6), likely due to the changing volume integrated in the HydraProbe's measurements. As the soil freezes, its permittivity decreases, and the integrated volume of the HydraProbe measurement increases, delaying the observation of the frozen condition by the sensor. It is also noteworthy that the total ice content in the soil column changes very little due to these short-duration freeze/thaw events. Generally we see a flattening of the slope during a midwinter melt (e.g. Figs. 5 and 6), where ice accumulation does not occur, however there is no clear evidence for significant ice loss during these events. It is difficult to establish the measured depth of thaw from the available field data, but there is no evidence that thaw extends beyond the first soil moisture and temperature sensor at a depth of 50 mm, limiting the anticipated ice loss to less than 25 mm given unsaturated soil conditions and a soil porosity not exceeding 0.5.

In this work, the depth of the buffer layer (85 mm) is specified based on the estimated zone of influence of the HydraProbe sensor to which the freeze/thaw data is compared. However, it is possible to specify other buffer layer thicknesses largely without compromising model efficacy in terms of total ice content estimation. For example, in the range of 10 mm to 7 mm, the change in reported ice content is less than 0.5%. Decreasing the buffer layer beyond 5 mm results in increasing error, growing from 2% at a 5 mm buffer layer, and resulting in model non-convergence for steep changes in surface temperature. When increasing the buffer layer thickness to more than 10 mm, model convergence issues also arise as this layer becomes too coarse to resolve short-duration events. For the mixed mineral soils in this study, the 8.5 mm buffer provided good agreement with field measurements, however for soils with higher porosity, it is likely that a shallower buffer layer be more suitable, whereas in lower porosity soils with high thermal conductivity, a thicker buffer layer may be more suitable to avoid issues related to the formation of extraneous near-surface freeze/thaw fronts.

4.4. Model evaluation: Freezing point

Figs. 5 and 6 also demonstrate that thaw occurs sooner in the interface model than in the extrapolated field data, though the interface model does accurately capture well over 90% of both the frozen and thawed data. It is thought that this is due to the single freezing point depression used to interpret the data. It is known that there is hysteresis in the freeze–thaw process, and that the freezing point temperature is generally lower than the thawing point (Saberi and Meschke, 2021). More work, including investigation of hysteretic behaviour in freeze/thaw modelling is needed, such as (Amiri and Craig, 2019) or the physical analysis of hysteresis, such as (Pardo Lara et al., 2021).

4.5. Model evaluation: Near-surface water content

The small difference in both freeze and thaw timing may also be driven by a mismatch in near-surface soil water content between simulated and observed. The error in estimated soil water content may arise because an equilibrium soil moisture profile is implemented in the interface model, as detailed in appendix C. The application of the model to mineral soils was expected to require a more complex representation of infiltration events including plug flow and moisture redistribution, but these were not found to be necessary in the reproduction of the freeze/thaw conditions in field observations of near-surface soils. The equilibrium assumption seems to be adequate for two reasons; first, the surface mass balance used is based on seasonal trends and is very smooth. This results in near-equilibrium moisture conditions in the soil column over most of the freeze/thaw season. Secondly, the parameter of interest is the frozen state of the near-surface soil. When mineral soils freeze, the impedance of ice in the soil pores is such that infiltration and evapotranspiration are negligible, and therefore these processes have little effect on the model results. This limitation of the model formulation may limit the model applicability in very low permeability clay soils subject to rapidly changing surface flux simulated on short timescales, and further analysis of the sensitivity of model results to these conditions would be needed to ensure the model is capable of resolving sub-hourly fluctuations in near-surface soil moisture for specific soil conditions of interest.

4.6. Model evaluation: Spring thaw

Measurements of spring thaw (and some midwinter events) yield small and rapid fluctuations in ice content in the surface layer. Spring temperatures in the Kenaston region have strong diurnal fluctuations, where the daytime temperature is well above the freezing point, but the overnight low is around - 1 °C. In the interface model, the near-surface ice content is estimated in the top 85 mm of soil, deemed equivalent

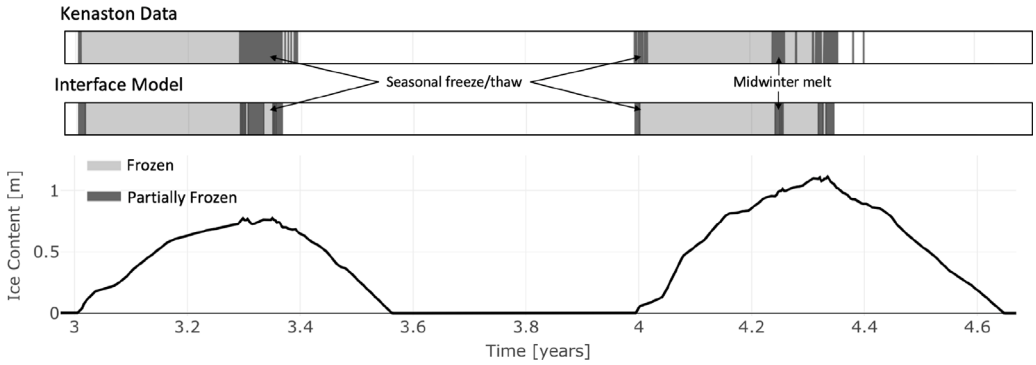

Fig. 5. Comparison of Kenaston field-data and interface model generated near-surface ice content indicating phase change (dark grey) and frozen soil (light grey). This 2 year subset (2016–2017) from 5 year simulation (2013–2018) drawn from Kenaston site 15. Seasonal freeze–thaw at the near surface occurs in fall and early spring, while a mid-winder melt event is highlighted in year 4. For this simulation, the overall agreement between freeze/thaw states was 94%, while the interface model correctly identified 95% of the frozen period.

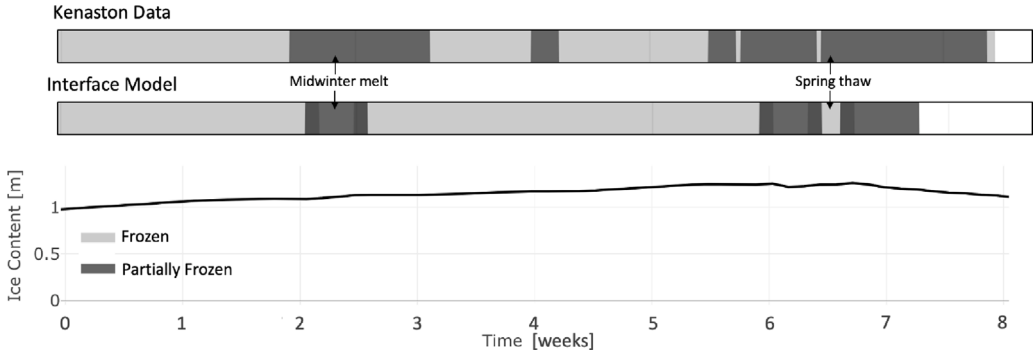

Fig. 6. Comparison of Kenaston field-data and interface model generated near-surface ice content indicating phase change (dark grey) and frozen soil (light grey). Interface model phase change takes less time, perhaps because of an under-estimate of the freezing point. Overall agreement between the freeze/thaw states is 94%, while the interface model correctly identifies 96% of the frozen period. Detail view from 5 year simulation drawn from Kenaston site 20.

to the depth of soil characterized by the field based freeze–thaw flag. This layer was included in the model as a mathematical construct to prevent the formation of very thin, non-physical frozen and thawed layers at the soil surface. With this layer, the interface model fails to capture some small-scale diurnal-fluctuation driven spring freeze/thaw events. However, these primarily occur when the underlying soil is frozen, and so the inability to track fractional ice content in the near-surface soil (especially when the ice content never freezes the pore water completely) likely has very little effect on the infiltration capacity and subsurface water movement. Water movement in the landscape is expected to be much more strongly affected by the fully frozen near-saturated layer at a depth of 10–15 cm below the soil surface. The relatively thin surface layer cannot store significant thermal energy, and the surface topography generally exceeds the scale of this layer, restricting the formation of flow pathways beyond the plot scale. As measured by the temperature sensors in the soil profile, short thaw events do not extend beyond the top 100 mm of soil, though this surface layer experiences temperature cycling and freeze/thaw throughout the winter as well as the shoulder seasons when strong diurnal temperature cycles are common. The increased freeze–thaw cycling can lead to changes in soil structure (Alkire and Morrison, 1983) and changes in decomposition of soil organic matter (Yanai et al., 2004). Further investigation is required to establish if this layer is physically significant across landscapes experiencing freeze–thaw.

The interface model is notably better at representing early fall freezing events (Fig. 7) which are of much higher hydrological importance as the underlying soil is ice-free and the surface (buffer) layer has the greatest impact on runoff partitioning. These results are promising for their potential improvement to runoff modelling.

4.7. Model transferability

Though the model configuration presented here is tuned to the specific field data available, the model is highly transferable given the availability of soil surface temperature data, approximate water flux, and general soil texture data. The model timing, total ice content, and depth of freezing are relatively insensitive to the choice of buffer layer thickness as long as this layer is thicker than 30 mm required to accommodate diurnal temperature fluctuations in shoulder seasons. The specific value of 85 mm chosen here was for comparison with data collected in the field. Further model comparison for peat soils containing permafrost are included in appendix E, demonstrating the model transferability to these soils.

4.8. Incorporation into hydrologic models

The ice content of the subsurface affects hydrologic processes predominantly through limiting the infiltrability and hydraulic conductivity of the soil, and altering the soil storage capacity. Though each of these properties is highly dependent on soil type and freeze–thaw history (Devoie et al., 2022), empirical relations are widely used to describe the impact of ice content on these relations (Chen et al., 2021). Recommendations are provided on how the interface model presented

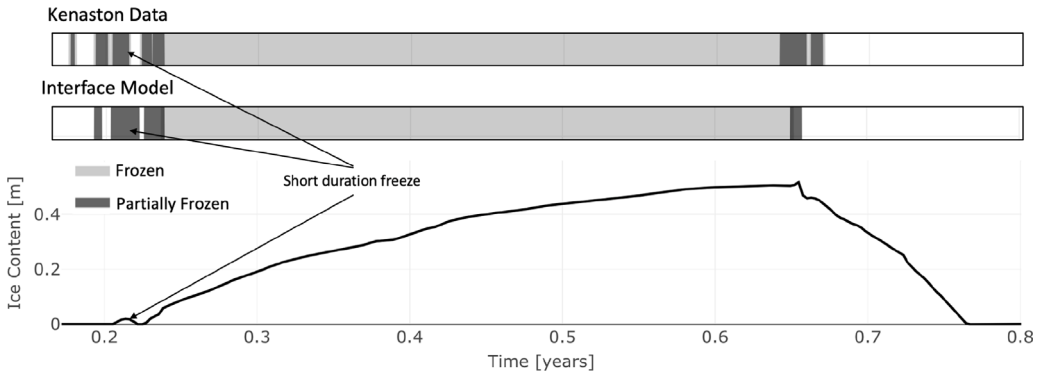

Fig. 7. Early season short-duration freeze/thaw event comparison between field-data and interface-model generated freeze/thaw. The overall agreement between freeze/thaw states was 95%, while the interface model correctly identified 96% of the frozen period. Single year of data drawn from 5 year simulation of Kenaston site 10.

here might be coupled with a hydrologic model to improve predictions under frozen conditions.

4.8.1. Hydraulic conductivity

It has been shown that for unsaturated conditions, or conditions in which there is no water available to move towards the freeze/thaw front, the ice segregation potential is low, and the hydraulic conductivity of the (partially) frozen soil is perhaps not equivalent to, but at least highly comparable with, the hydraulic conductivity of the unsaturated soil with equivalent water content (Kurylyk and Watanabe, 2013; Watanabe and Osada, 2017; Cheng et al., 2023). However, in soils that permit movement of water towards the freeze/thaw front, and especially in those where the formation of segregated ice is possible, a drastic reduction in hydraulic conductivity is observed with ice formation (Burt and Williams, 1976; Watanabe and Wake, 2008; Chen and Zhang, 2020; Cheng et al., 2023). This decrease in conductivity is especially notable in soils where pore water occupies capillary space (SLS soils) as opposed to soils dominated by adsorbed water (SS soils), while the range of soils between SS and SLS show a range of impedance effects which are difficult to estimate (Koopmans and Miller, 1966; Azmatch et al., 2012). Many relations exist to predict the hydraulic conductivity of frozen soils based on their temperature, and further research is needed to determine which relations are widely applicable to soils and which are soil-specific. Lacking this work, we present an example relation form Tarnawski and Wagner (1996), which was developed for any soil with log-normally distributed grain size, but only tested on sand. Though recent work applying ice segregation theory may yield more accurate and versatile results (e.g Cheng et al. (2023)), the relations described are prohibitively complex, and require more input data than is available, and will not be used for the proof of concept shown here. According to Tarnawski and Wagner (1996), the hydraulic conductivity of partially frozen soils can be given by k:

$$k = K_{sat}\left(\frac{\theta_{un}}{\theta_{sat}}\right)^{2b+3} \tag{1}$$

$$b = \exp\left(m_{cl}\ln d_{cl} + m_{si}\ln d_{si} + m_{sa}\ln d_{sa}\right)^{-0.5} + 0.2\cdot\exp\left[\Sigma_1^3 m_i(lnd_i)^2 - \left(\Sigma_1^3 m_i \ln d_i\right)^2\right]^{0.5}$$

Where K_{sat} is the saturated hydraulic conductivity, θ_{un} is the unfrozen water content (volumetric), and b is a fitting parameter based on soil texture, in which m_{cl}, m_{si}, and m_{sa} are clay, silt, and sand mass fractions, and d_x are the particle size ranges used to separate the clay, sand and silt ranges (typically d_{cl} = 0.001 mm, d_{si} = 0.026 mm, and d_{sa} = 1.025 mm) (Tarnawski and Wagner, 1996).

The interface model reports a binary froze/thawed state for the soil, making θ_{un} a potentially un-interesting parameter. However it also reports a bulk soil temperature, which alongside the SFCC for a particular soil (estimated using the repository of SFCCs presented in Devoie et al. (2022)), can be used to estimate the bulk unfrozen water content:

$$\theta_{un} = \bar{\theta}\left(1 - \left(\frac{T_f - T}{273.15 + T_f}\right)^{\beta}\right) \tag{2}$$

This strategy addresses the challenge posed by the interface model reporting a binary frozen/thawed state as opposed to the exact ice content, and due to the verified conservation of energy in the model, the average temperature of the frozen layer is a largely accurate measure. From this estimation of unfrozen water content, it is then possible to determine the hydraulic conductivity using Eq. (1) based on the soil properties. Due to the fully frozen nature of the interface model, the temperature reported is likely colder than the actual temperature, leading to a conservative estimate of permeability.

If this scheme were applied to Kenaston site 15 (shown in Fig. 5), the resulting infiltrability is reported in Fig. 8. The specified flux at the soil surface is included in this figure, and any region in which the infiltration supplied at the surface exceeds the infiltrability of the soil is shaded in blue. This occurs in the thawing season of the simulation, where the soil is recovering to its maximum infiltrability as ground ice melts in the late spring. While both infiltration and runoff data were not collected at this study site, this proof of concept points to a need for further field validation datasets for frozen conditions.

4.8.2. Infiltration and storage

Infiltration refers to water entering a soil column vertically, and is closely related to the hydraulic conductivity of the soil, but is complicated by the predominantly laterally layered structure of soils, the maximum storage of the system, and vertical temperature and moisture gradients (Dingman, 2015). These gradients often result in the formation of ice rich and ice poor layers, and can even lead to the development of segregated ground ice (layers of pure ice in a soil column formed during freezing) (Zhao and Gray, 1999; Woo, 2012). The infiltrability, or capacity for infiltration of a soil, depends on its layered structure, ice content, and total saturation which determine the soil's vertical hydraulic conductivity. Infiltration is typically limited either by the speed of infiltration as determined by the vertical hydraulic conductivity, or by the total capacity of the soil to receive infiltration - i.e. the void space available to store the additional water (Dingman, 2015). If the rate of water delivery to the soil surface is faster than can enter the soil as limited by the hydraulic conductivity, ponding at the soil surface will occur, and if the air temperature is sub-zero this is likely to lead to the formation of ice at the soil surface, and a cessation of infiltration entirely. If the water is delivered to the soil surface at a rate which can be accepted into the soil, then the total available porosity to receive water must be considered.

The infiltration capacity may be artificially limited in frozen soils either by the presence or formation of ice in pore spaces or as lenses.

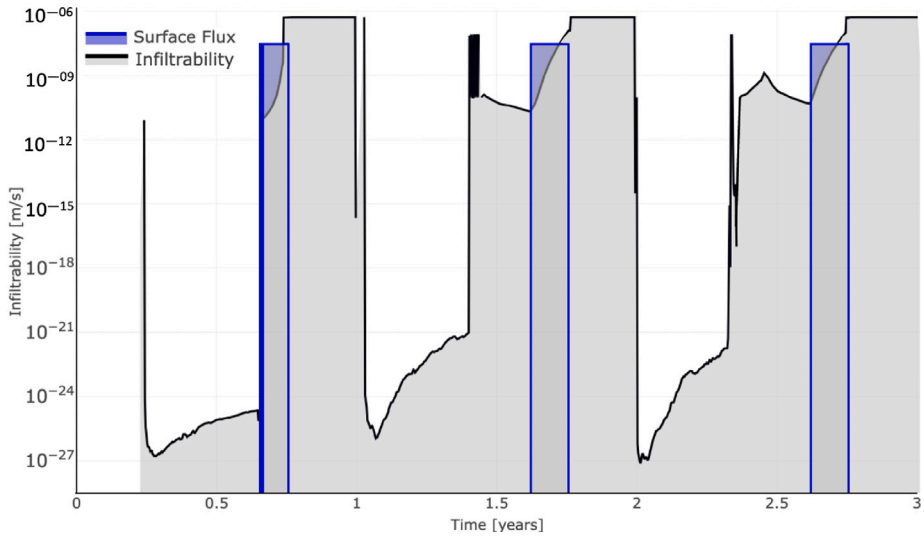

Fig. 8. Comparison between the imposed surface flux (in blue) and the modelled infiltrability of the soil (shaded in grey). The region where the specified flux exceeds the infiltration is shaded in blue, and corresponds to late spring infiltration excess runoff generation.

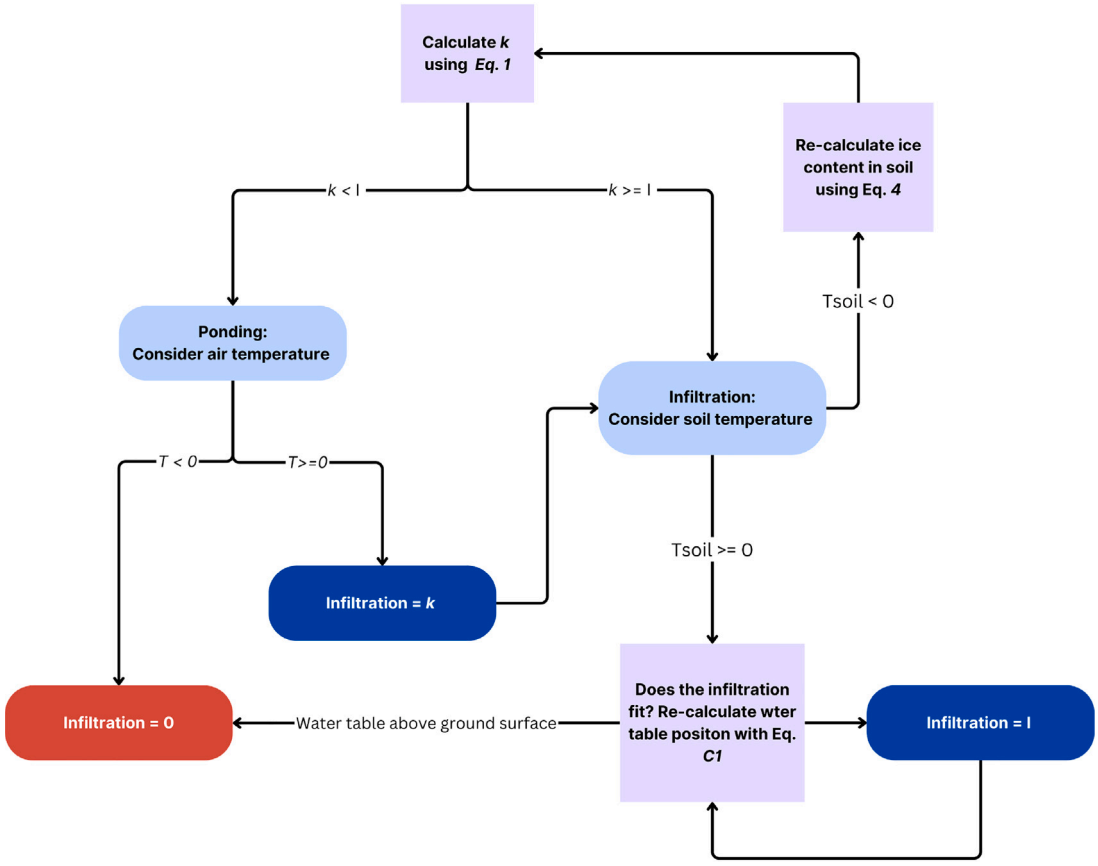

Fig. 9. Flow chart describing the evaluation of infiltration into frozen soils.

Ice formation is common when infiltration occurs into soils with a temperature notably below 0 °C. In these cases, the degree of ice formation can be estimated by converting the 'cold content' of the soil calculated using Eq. (3). In this relation $\Delta\theta_I$ describes the change in ice content in the profile, $\bar{T}$ is the bulk (sub-zero) soil temperature, C_p is the bulk heat capacity calculated using Equation D3, Z is the depth of the frozen layer, and L_f is the latent heat of fusion. Once applied the bulk temperature, $\bar{T} = 0$ °C.

$$\Delta\theta_I = \frac{\bar{T}\bar{C}_p Z}{L_f} \tag{3}$$

Given these competing processes, as well as the physics governing ice lens formation not discussed here (Konrad and Morgenstern, 1980),

estimating the infiltrability of freezing soils is challenging. We provide one of several options in Fig. 9 as an example implementation.

The total change in storage in the soil column is described in appendix C, which assumes an equilibrium water table position. The above flow chart describes the interaction between mass storage and energy storage in freezing soils, as it is implemented in the presented interface model. Given specified groundwater fluxes from hydrologic models, this can be used to update over-winter conditions for more appropriate representation of spring melt, as well as mid-winter infiltration events.

5. Conclusions

An interface model was presented to simulate the position of the freezing front in variably saturated soils undergoing freeze/thaw processes. This model has been demonstrated to efficiently and stably reproduce the timing and magnitude of freeze/thaw events both on the inter-annual scale as well as on the sub-daily scale when compared to both a high-resolution finite volume model and to data collected at a site in Southern Saskatchewan. The interface model fills a utility gap between computationally intensive physically-based continuum models and low-fidelity empirical expressions for ground freeze–thaw, and its computational expediency makes it suitable for integration into practical forecasting tools. Methods for the interpretation of storage capacity and permeability from this model are presented for ease of incorporating it into hydrologic models. Such a contribution is especially relevant in areas such as the Canadian prairies where an increase in midwinter freeze/thaw events of short duration is limiting the predictive ability of current hydrologic models.

Limitations of the presented interface model include a restriction to relatively coarse grained materials as the model does not include an SFCC, instead tracking a sharp freeze/thaw interface, and does not include the formation of segregated ground ice. Further work incorporating a linear SFCC into the analytical solution would in part resolve this shortcoming, however the analytical solution would not permit other more complex functional forms of an SFCC. Work is underway to incorporate the interface model presented here into the Raven Hydrological Modelling Framework, and it is hoped that results will show improved representation of hydrology in cold regions.

CRediT authorship contribution statement

Élise G. Devoie: Writing – review & editing, Writing – original draft, Visualization, Validation, Methodology, Investigation, Formal analysis, Data curation, Conceptualization. **Renato Pardo Lara:** Writing – review & editing, Data curation. **Aaron Berg:** Writing – review & editing, Data curation. **William L. Quinton:** Writing – review & editing, Data curation. **James R. Craig:** Writing – review & editing, Supervision, Resources, Methodology, Funding acquisition, Conceptualization.

Declaration of competing interest

The authors declare that they have no known competing financial interests or personal relationships that could have appeared to influence the work reported in this paper.

Acknowledgements

We acknowledge the funding support provided by NSERC and CIFAR. We acknowledge the Liidlii Kue First Nation and the Jean Marie River First Nation for their continued support of the SCRS. We acknowledge the generous support of the Government of the Northwest Territories through their partnership agreement with Wilfrid Laurier University and of the Cold Regions Research Centre. We also acknowledge the support from ArcticNet through their support of the Dehcho Collaborative on Permafrost (DCoP).

Appendix A. Supplementary data

Supplementary material related to this article can be found online at https://doi.org/10.1016/j.envsoft.2025.106816.

Data availability

Name of the software: InterfaceModel

Developer: Élise Devoie [aut, cre], James R. Craig [ctb]. Contact information: elise.devoie@queensu.ca.

Year first available: 2022.

Hardware requirements: PC/Mac.

Software requirements: Matlab.

Programming language: Matlab.

Program size: 111 kb.

Software availability: https://github.com/egdevoie/InterfaceModel.git

License: MIT License (https://opensource.org/license/mit)

The data that support the findings of this study are openly available in the Federated Research Repository at https://doi.org/10.20383/101.0116.

Size of archive: 903.25 MB.

References

Alkire, B.D., Morrison, J.M., 1983. Change in soil structure due to freeze-thaw and repeated loading. Transp. Res. Rec. (918).

Amiri, E.A., Craig, J.R., 2019. Effect of soil thermal heterogeneity on permafrost evolution. chapter 1. pp. 492–499. http://dx.doi.org/10.1061/9780784482599.057.

Azmatch, T.F., Sego, D.C., Arenson, L.U., Biggar, K.W., 2012. Using soil freezing characteristic curve to estimate the hydraulic conductivity function of partially frozen soils. Cold Reg. Sci. & Technol. 83–84, 103–109. http://dx.doi.org/10.1016/j.coldregions.2012.07.002.

Burns, T.T., Berg, A.A., Cockburn, J., Tetlock, E., 2016. Regional scale spatial and temporal variability of soil moisture in a prairie region. Hydrol. Process. 30 (20), 3639–3649.

Burt, T., Williams, P.J., 1976. Hydraulic conductivity in frozen soils. Earth Surf. Process. 1 (4), 349–360.

Chen, J., Mei, S., Rempel, A.W., 2021. Estimating permeability of partially frozen soil using floating random walks. Water Resour. Res. 57, http://dx.doi.org/10.1029/2021WR030598.

Chen, L., Zhang, X., 2020. A model for predicting the hydraulic conductivity of warm saturated frozen soil. Build. Environ. 179, 106939.

Cheng, S.-H., Engel, B.A., Liu, R., Wu, H.-X., Wang, Y.-B., 2023. Impedance factor of hydraulic conductivity for frozen soil based on ice segregation theory and its application. Water Resour. Res. 59, http://dx.doi.org/10.1029/2022wr033876.

Cuntz, M., Haverd, V., 2018. Physically accurate soil freeze-thaw processes in a global land surface scheme. J. Adv. Model. Earth Syst. 10 (1), 54–77.

Devoie, É.G., Craig, J.R., 2020. A semianalytical interface model of soil freeze/thaw and permafrost evolution. Water Resour. Res. 56 (8), http://dx.doi.org/10.1029/2020WR027638.

Devoie, É.G., Craig, J.R., Connon, R.F., Quinton, W.L., 2019. Taliks: A tipping point in discontinuous permafrost degradation in peatlands. Water Resour. Res. 55 (11), 9838–9857. http://dx.doi.org/10.1029/2018WR024488.

Devoie, É., Gruber, S., McKenzie, J.M., 2022. A repository of measured soil freezing characteristic curves: 1921 to 2021. Earth Syst. Sci. Data 14 (7), 3365–3377. http://dx.doi.org/10.5194/essd-14-3365-2022, URL https://essd.copernicus.org/articles/14/3365/2022/.

Diersch, H.J.G., 2013. FEFLOW: Finite Element Modeling of Flow, Mass and Heat Transport in Porous and Fractured Media. Springer Science & Business Media.

Dingman, S.L., 2015. Physical Hydrology. Waveland Press.

Fox, J.D., 1992. Incorporating freeze-thaw calculations into a water balance model. Water Resour. Res. 28 (9), 2229–2244. http://dx.doi.org/10.1029/92WR00983.

Granger, R., Gray, D., Dyck, G., 1984. Snowmelt infiltration to frozen prairie soils. Can. J. Earth Sci. 21 (6), 669–677.

Grenier, C., Régnier, D., Mouche, E., Benabderrahmane, H., Costard, F., Davy, P., 2013. Impact of permafrost development on groundwater flow patterns: a numerical study considering freezing cycles on a two-dimensional vertical cut through a generic river-plain system. Hydrogeol. J. 21 (1), 257–270.

Hayashi, M., 2013. The cold vadose zone: Hydrological and ecological significance of frozen-soil processes. Vadose Zone J. 12 (4), vzj2013–03.

Hayashi, M., Goeller, N., Quinton, W.L., Wright, N., 2007. A simple heat-conduction method for simulating the frost-table depth in hydrological models. Hydrol. Process. 2610–2622. http://dx.doi.org/10.1002/hyp.6792.

Hinkel, K.M., Nicholas, J.R.J., 1995. Active layer thaw rate at a boreal forest site in Central Alaska, U.S.A.. Arct. Alp. Res. 27 (1), 72–80, URL http://www.jstor.org/stable/1552069.

Hyman-Rabeler, K.A., Loheide, S.P., 2023. Drivers of variation in winter and spring groundwater recharge: Impacts of midwinter melt events and subsequent freezeback. Water Resour. Res. 59 (1), e2022WR032733.

Van der Kamp, G., Hayashi, M., Gallen, D., 2003. Comparing the hydrology of grassed and cultivated catchments in the semi-arid Canadian prairies. Hydrol. Process. 17 (3), 559–575.

Konrad, J.M., Morgenstern, N.R., 1980. A mechanistic theory of ice lens formation in fine-grained soils. Can. Geotech. J. 17 (4), 473–486.

Koopmans, R.W.R., Miller, R.D., 1966. Soil freezing and soil water characteristic curves. Soil Sci. Am. J. 30 (6), 680–685. http://dx.doi.org/10.2136/sssaj1966.03615995003000060011x.

Kurylyk, B., Watanabe, K., 2013. The mathematical representation of freezing and thawing processes in variably-saturated, non-deformable soils. Adv. Water Resour. 60, 160–177.

Lundin, L.C., 1990. Hydraulic properties in an operational model of frozen soil. J. Hydrol. 118 (1–4), 289–310.

Luo, L., Robock, A., Vinnikov, K.Y., Schlosser, C.A., Slater, A.G., Boone, A., Etchevers, P., Habets, F., Noilhan, J., Braden, H., et al., 2003. Effects of frozen soil on soil temperature, spring infiltration, and runoff: Results from the PILPS 2 (d) experiment at Valdai, Russia. J. Hydrometeorol. 4 (2), 334–351.

Majorowicz, J., Grasby, S.E., 2021. Deep geothermal heating potential for the communities of the western Canadian sedimentary basin. Energies 14 (3), http://dx.doi.org/10.3390/en14030706.

McKenzie, J.M., Voss, C.I., Siegel, D.I., 2007. Groundwater flow with energy transport and water–ice phase change: Numerical simulations, benchmarks, and application to freezing in peat bogs. Adv. Water Resour. 30 (4), 966–983.

Meteorological Service of Canada, 2012. National climate data archive of Canada. Government of Canada, URL http://www.climate.weather.gc.ca.

Mohammed, A.A., Pavlovskii, I., Cey, E.E., Hayashi, M., 2019. Effects of preferential flow on snowmelt partitioning and groundwater recharge in frozen soils. Hydrol. Earth Syst. Sci. 23 (12), 5017–5031.

Molson, J., Frind, E., 2015. HEATFLOW–SMOKER version 7.0-density-dependent flow and advective-dispersive transport of thermal energy, mass or residence time in three-dimensional porous or discretely-fractured porous media. Manuscr. UniversitÉ Laval.

Niu, G.Y., Yang, Z.-L., 2006. Effects of frozen soil on snowmelt runoff and soil water storage at a continental scale. J. Hydrometeorol. 7 (5), 937–952.

Pardo Lara, R., Berg, A., Warland, J., Parkin, G., 2021. Implications of measurement metrics on soil freezing curves: A 1 simulation of freeze-thaw hysteresis. Preprint.

Pardo Lara, R., Berg, A., Warland, J., Tetlock, E., 2020. In situ estimates of freezing/melting point depression in agricultural soils using permittivity and temperature measurements. Water Resour. Res. 56 (5), e2019WR026020.

Pavlovskii, I., Hayashi, M., Itenfisu, D., 2019. Midwinter melts in the Canadian prairies: energy balance and hydrological effects. Hydrol. Earth Syst. Sci. 23 (4), 1867–1883.

Pomeroy, J., Gray, D., Brown, T., Hedstrom, N., Quinton, W.L., Granger, R., Carey, S., 2007. The cold regions hydrological model: a platform for basing process representation and model structure on physical evidence. Hydrol. Process.: An Int. J. 21 (19), 2650–2667.

Pörtner, H.O., Roberts, D., Masson-Delmotte, V., Zhai, P., Tignor, M., Poloczanska, E., Mintenbeck, K., Alegría, A., Nicolai, M., Okem, A., Petzold, J., Rama, B., Weyer, N., 2019. IPCC, 2019: IPCC Special Report on the Ocean and Cryosphere in a Changing Climate. Intergovernmental Pannel on Climate Change.

Qi, J., Zhang, X., Wang, Q., 2019. Improving hydrological simulation in the upper mississippi river basin through enhanced freeze-thaw cycle representation. J. Hydrol. 571, 605–618.

Rühaak, W., Anbergen, H., Grenier, C., McKenzie, J., Kurylyk, B.L., Molson, J., Roux, N., Sass, I., 2015. Benchmarking numerical freeze/thaw models. Energy Procedia 76, 301–310.

Saberi, P.S., Meschke, G., 2021. A hysteresis model for the unfrozen liquid content in freezing porous media. Comput. Geotech. 134, http://dx.doi.org/10.1016/j.compgeo.2021.104048.

Seyfried, M.S., Murdock, M.D., 2004. Measurement of soil water content with a 50-MHz soil dielectric sensor. Soil Sci. Am. J. 68 (2), 394–403. http://dx.doi.org/10.2136/sssaj2004.3940.

Shaw, R.J., Hendry, M.J., 1998. Hydrogeology of a thick clay till and cretaceous clay sequence, Saskatchewan, Canada. Can. Geotech. J. 35 (6), 1041–1052. http://dx.doi.org/10.1139/t98-060.

Shook, K., Pomeroy, J., Spence, C., Boychuk, L., 2013. Storage dynamics simulations in prairie wetland hydrology models: Evaluation and parameterization. Hydrol. Process. 27 (13), 1875–1889.

Slater, A., Pitman, A., Desborough, C., 1998. Simulation of freeze-thaw cycles in a general circulation model land surface scheme. J. Geophys. Res.: Atmospheres 103 (D10), 11303–11312.

Tarnawski, V.R., Wagner, B., 1996. On the prediction of hydraulic conductivity of frozen soils. Can. Geotech. J. 33 (1), 176–180.

Tetlock, E., Toth, B., Berg, A., Rowlandson, T., Ambadan, J.T., 2019. An 11-year (2007–2017) soil moisture and precipitation dataset from the Kenaston Network in the Brightwater Creek basin, Saskatchewan, Canada. Earth Syst. Sci. Data 11 (2), 787–796.

Verseghy, D.L., 2000. The Canadian land surface scheme (CLASS): Its history and future. Atmos.-Ocean 38 (1), 1–13. http://dx.doi.org/10.1080/07055900.2000.9649637.

Wang, L., Koike, T., Yang, K., Jin, R., Li, H., 2010. Frozen soil parameterization in a distributed biosphere hydrological model. Hydrol. Earth Syst. Sci. 14 (3), 557–571.

Wang, W., Rinke, A., Moore, J.C., Ji, D., Cui, X., Peng, S., Lawrence, D.M., McGuire, A.D., Burke, E.J., Chen, X., Decharme, B., Koven, C., MacDougall, A., Saito, K., Zhang, W., Alkama, R., Bohn, T.J., Ciais, P., Delire, C., Gouttevin, I., Hajima, T., Krinner, G., Lettenmaier, D.P., Miller, P.A., Smith, B., Sueyoshi, T., Sherstiukov, A.B., 2016. Evaluation of air–soil temperature relationships simulated by land surface models during winter across the permafrost region. Cryosphere 10 (4), 1721–1737. http://dx.doi.org/10.5194/tc-10-1721-2016, URL https://tc.copernicus.org/articles/10/1721/2016/.

Wang, L., Zhou, J., Qi, J., Sun, L., Yang, K., Tian, L., Lin, Y., Liu, W., Shrestha, M., Xue, Y., et al., 2017. Development of a land surface model with coupled snow and frozen soil physics. Water Resour. Res. 53 (6), 5085–5103.

Watanabe, K., Osada, Y., 2017. Simultaneous measurement of unfrozen water content and hydraulic conductivity of partially frozen soil near 0 °C. Cold Reg. Sci. & Technol. 142, 79–84. http://dx.doi.org/10.1016/j.coldregions.2017.08.002.

Watanabe, K., Wake, T., 2008. Hydraulic conductivity in frozen unsaturated soil. In: Proceedings of the 9th International Conference on Permafrost. vol. 29, Univ. of Alaska Fairbanks Fairbanks, Alaska, pp. 1927–1932.

Williams, C.M., Henry, H.A., Sinclair, B.J., 2015. Cold truths: how winter drives responses of terrestrial organisms to climate change. Biological Rev. 90 (1), 214–235. http://dx.doi.org/10.1111/brv.12105.

Wittrock, V., Dunn, S., 2016. Climate reference station saskatoon annual summary 2016. Prov. Od Sask..

Woo, M.k., 2012. Permafrost Hydrology. Springer Science & Business Media.

Woo, M.K., Arain, M., Mollinga, M., Yi, S., 2004. A two-directional freeze and thaw algorithm for hydrologic and land surface modelling. Geophys. Res. Lett. 31 (12).

Yanai, Y., Toyota, K., Okazaki, M., 2004. Effects of successive soil freeze-thaw cycles on soil microbial biomass and organic matter decomposition potential of soils. Soil Sci. Plant Nutr. 50 (6), 821–829.

Yi, S., Arain, M.A., Woo, M.K., 2006. Modifications of a land surface scheme for improved simulation of ground freeze-thaw in northern environments. Geophys. Res. Lett. 33 (13).

Zhao, L., Gray, D., 1999. Estimating snowmelt infiltration into frozen soils. Hydrol. Process. 13 (12–13), 1827–1842.